Magazine of Civil Engineering. 2019. 89(5). Pp. 115–128
Инженерно-строительный журнал. 2019. № 5(89). С. 115–128

Magazine of Civil Engineering

ISSN 2071-0305

journal homepage: http://engstroy.spbstu.ru/

DOI: 10.18720/MCE.89.10

Coordinate functions quadratic approximation in V.I. Slivker's semi-shear stability theory

V.A. Rybakov, V.V. Lalin, S.S. Ivanov, A.A. Azarov*
Peter the Great St. Petersburg Polytechnic University, St. Petersburg, Russia
** E-mail: alexio009@mail.ru*

Keywords: thin-walled bars, Slivker's semi-shear theory, stability theory, stability functional, Hermite polynomial, coordinate functions

Abstract. The loss of bearing capacity of some compressed self-framing metal structures elements occurs with a general buckling and for some of them there is no analytical solution. That is why consideration of the problem variational statement and its numerical solution is particular interesting. In this study, the stiffness and geometric stiffness matrices were obtained for Hermite polynomials quadratic variation that approximate the functions of the twist angle and deplanation functions. The dependences of the critical load on the number of finite elements for different geometric and kinematic boundary conditions are obtained. The inconsistency of the approximation by forms linear functions is shown in comparison with the quadratic approximation, which turns out to be optimal. The reason is that it almost immediately reaches the exact analytical solution, with a flexural-torsional form of buckling. For a purely torsional or flexural form of buckling, it is shown that functions of the twist angle and deplanation functions approximation for different Hermite polynomials does not give faster convergence.

1. Introduction

The evaluation of the building structures reliability is the main task in civil engineering. So, in [1] authors considered the applying of probabilistic method for bearing capacity criterion estimation. Planar frame rod model was presented in [2–3]. They determined forces equations in the most compressed elements, depending upon the amount of panels in grid. This has enabled elements strength [4] and general stability determination. However, this kind of Self-framing metal application in frame constructions must have a strict evidence. So in [5] they showed the benefits of using Self-framing metal for pitched roofs major repairs.

In [6] they analyzed buckling modes depending on various cases of the rod stress state and its geometrical and physical characteristics. Stability losses bending modes of axially-loaded bars depend on the face sections stiffness correlation. After the study of flexural-torsional stability losses modes of the non-axially compressed, variable stiffness, constant chords width I-shaped bars the following was found. Bending modes for bars with any unilateral end-point eccentricity combination and same chords slopes are not differ significantly; they might be taken to be equal. However, torsional modes are very different, they depend on the chords slopes. The study of bending-torsional buckling modes of variable stiffness non-axially compressed I-shaped beams which have different chords width and high, showed: modes depend on chord slope and narrowing combination. Constraint of warping impact on the critical force and the buckling mode. In [7], the deformation calculation and eccentric stability with eccentricity around two axes, compressed combined section bars, taking into account the warping links, were investigated. This study is based on the equations proposed by E.A. Beilin. The differential equations system solution by combining exact integration methods with the Bubnov-Galerkin's method with exact satisfaction of different boundary conditions shows us the reason to use a Self-framing metal bar compressed with a biaxial eccentricity. It is confirmed that in the particular case of the cross section geometry and the application of a longitudinal load, a bifurcation of the equilibrium modes is possible and the problem of compression with biaxial eccentricity in general form is not bifurcation. The problem of deformation and calculation for the arbitrary profile bar stability of with warping

Rybakov, V.A., Lalin, V.V., Ivanov, S.S., Azarov, A.A. Coordinate functions quadratic approximation in V.I. Slivker's semi-shear stability theory. Magazine of Civil Engineering. 2019. 89(5). Pp. 115–128. DOI: 10.18720/MCE.89.10

Рыбаков В.А., Лалин В.В., Иванов С.С., Азаров А.А. Квадратичная аппроксимация функций форм в полусдвиговой теории устойчивости В.И. Сливкера // Инженерно-строительный журнал. 2019. № 5(89). С. 115–128. DOI: 10.18720/MCE.89.10

bonds distributed along the length is investigated, and a change in displacements and forces is revealed depending on the compliance of the warping links. A natural study of combined profile warping connections bars constrained torsion was carried out. The difference between experiment and the analytical solution is 16 % Methods for approximating the local and general buckling modes and cross section stability, with perforations, were provided in [8–9]. According to the results, the total loss of stability of elements with holes can be approximated by applying a "weighted-average" approach in determining the geometric characteristics of the section. The loss of the local shape of the stability of elements with holes is approximated using careful modifications of the models of the end strips of the cross section. Since the hole effect is different, in each case of buckling new model is required. In [10], the stability of the cross-sectional shape depending on the load is investigated using the example of monosymmetric I-beams. According to the results, the nature of buckling changes with a change in the length of the monosymmetric I-beam. In [11–12], the features of determining the bearing capacity of Self-framing metal structures are considered using the North American design standards and Eurocode 3. A loss of local stability in the both standards is taken into account equally, by the effective cross section. These standards are based on the methods for determining the parts of the section that are turned off from work because of the secondary buckling.

Works on numerical methods for calculating Self-framing metal bars.

The practical contribution was made in the works [13–15], where, based on the core model of calculation, analytical solutions for the displacement functions and internal force factors according to the semi-shear theory by V.I. Slivker were given. Solutions are given for three most popular structures that are often encountered in practice with kinematic boundary conditions given in the paper, i.e. practically determine the field of the stress-strain state (SSS). Finite elements of three types are constructed for the numerical solution of the constrained torsion of Self-framing metal bars problem in a variation formulation using the Ritz method with approximating polynomials of the chosen order according to V.I. Slivker's semi-shear theory. Iterative calculations were carried out, and then recommendations were given on choosing the sizes of finite elements depending on the type of the finite element and its interpolation polynomials. A database was created for correlation of the open and / or closed profile form for displacement and internal force factors.

The system of equations of the dynamics [16] of a Self-framing metal bar for the theory by V.I. Slivker was derived. In this system: one equation describes only longitudinal vibrations, while the remaining system of joint equations describes flexural-torsional warping oscillations. The dispersion dependences and phase velocities of torsional-warping waves in bisymmetric. Self-framing metal bar was analyzed according to the theory by V.I. Slivker. As a consequence, it was possible to conclude about the second optical dispersion branch, which, according to analysis of the eigenmodes of oscillations, corresponds to high-frequency warping oscillations. The formula was obtained that approximates the frequency of warping oscillations and the formula that determines the lowest frequency. Also matrices of masses were agreed, which differ in the type of displacement functions approximation, the twist angle functions of the warping measures for solving static problems with any kinematic boundary conditions. It certainly has great practical use. The automated algorithm has been developed for solving the spatial structures of Self-framing metal elements of both a closed and open profile in a dynamic formulation.

In the paper [17–18], stiffness matrices for various types of approximation of displacement functions with different numbers of freedom degrees of finite elements were determined. The greatest value in the operation of structures is the justification for taking into account nodal stiffness, compliance, or taking into account initial imperfections when calculating Self-framing metal bars for strength and stability. For example, [19] is about taking into account the initial imperfections of tubular nodal on their bearing capacity. The results showed the possibility of neglecting the negative effects caused by geometric imperfections during the operation of the structure. Influence of knot stiffness on the Self-framing metal rods stability were considered in [20]. The influence of the torsional stiffness of the beam-wall connection and the dependence of these characteristics on the number of floors of the rack were noted. In fact, the nodal mates of crossbars with columns occupy some intermediate value, which has a certain compliance, the magnitude of which is influenced by the constructive nodal solution. The work [21] shows the need to use the scheme with nodes that perceive some of the bending moments.

In [22], the bifurcation stability problem was solved numerically, much of which was written on solving it, including [23–25], a thin-walled rod on the Vlasov's theory and analytically on the Euler's theory. A significant difference was revealed in the value of the critical load according to two theories, a greater value is obtained by numerical calculation using the V.Z. Vlasov's no-slip theory.

In [26] they consider the stability of straightened from the plane thin-walled cold-formed beams with two types of finite element models. They took into account the geometric nonlinearity and material properties which were built in the ABAQUS software package. Model with two elements: two beams, through panels and hot-rolled pipes. Model with one element: one beam, and the other component, which was designed using the appropriate boundary conditions. It was found that the results for the two models are similar, but the simplified model is certainly computationally more attractive. It was also found that strain hardening does not affect the behavior of cold-formed beams.

This research is a continuation of the work [27] on the application of the finite element method in solving problems of stability of thin-walled rods according to the semi-shear theory by V.I. Slivker [23, 24].

A stiffness matrix and a geometric stiffness matrix for a quadratic approximation of the torsion functions and the warping measure were obtained in this research. Several problems with different forms of buckling are considered, the problem domain is defined in which approximation of torsion functions and warping measures by quadratic functions are faster than approximation by linear Hermite polynomials used in [27].

2. Methods

Equilibrium stability functional of a squeezed-curved thin-walled rod according to a semi-shear theory by V.I. Slivker [27]:

$$S = \frac{1}{2}\int_0^L [GI_x\theta'^2 + GI_\beta(\theta' - \beta)^2 + EI_z\eta''^2 + EI_y\zeta''^2 + EI_\omega\beta'^2 + K\theta'^2 + N(\eta'^2 + \zeta'^2) + \\ + 2(M_\eta\eta'' - M_\zeta\zeta'')\theta]dx. \quad (1)$$

A detailed description of the functional integrand is presented in the previous article [27]:

Consider the i-th finite element of a thin-walled rod:

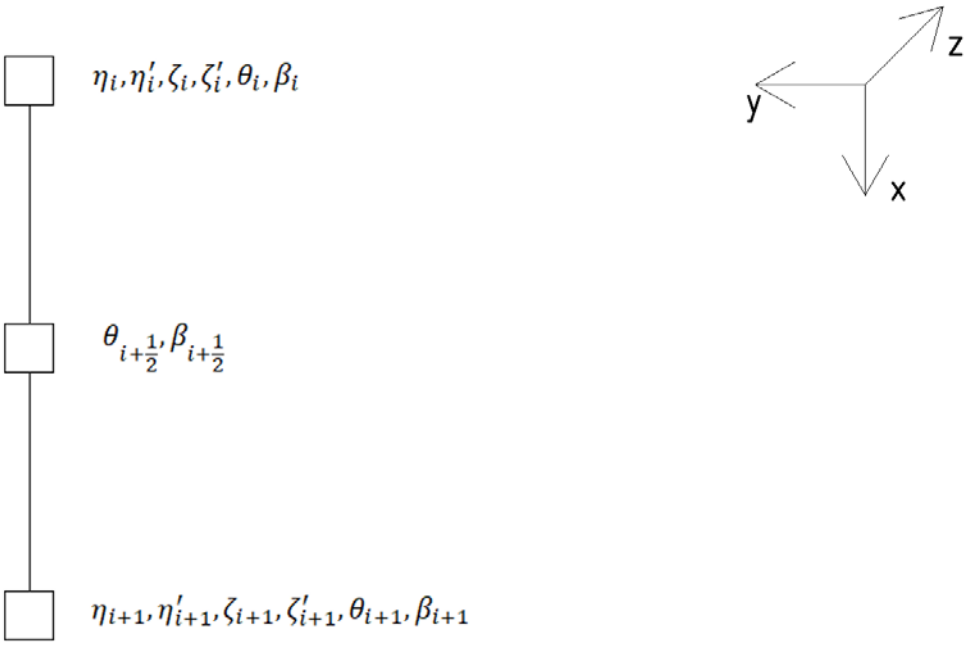

Figure 1. Finite element with 14 degrees of freedom.

Nodal displacements of a single finite element column:

$$U = \left(\eta_i \;\; \eta_i' \;\; \xi_i \;\; \xi_i' \;\; \theta_i \;\; \beta_i \;\; \theta_{i+\frac{1}{2}} \;\; \beta_{i+\frac{1}{2}} \;\; \eta_{i+1} \;\; \eta_{i+1}' \;\; \xi_{i+1} \;\; \xi_{i+1}' \;\; \theta_{i+1} \;\; \beta_{i+1} \right)^T, \quad (2)$$

where η is bending center movement along Y;

η' is rotation angle about the axis Z;

ζ is bending center movement along Z;

ζ' is rotation angle about the axis Y;

θ is torsion angle;

β is warping measure in the corresponding nodes.

We write the functional V.I. Sliver in the matrix form, the process is given in [27]:

$$S=\frac{1}{2}\int_0^L\{GI_x[U_\theta]^T[H']_{\theta\beta}^T[H']_{\theta\beta}[U_\theta]+GI_\beta[U_{\theta\beta}]^T[\Phi]^T[\Phi][U_{\theta\beta}]+$$
$$+EI_z[U_\eta]^T[H'']_{\eta\zeta}^T[H'']_{\eta\zeta}[U_\eta]+EI_y[U_\zeta]^T[H'']_{\eta\zeta}^T[H'']_{\eta\zeta}[U_\zeta]+$$
$$+EI_\omega[U_\beta]^T[H']_{\theta\beta}^T[H']_{\theta\beta}[U_\beta]-P[(r_p^2+e_zb_z+e_yb_y+\omega_Ab_\omega)[U_\theta]^T[H']_{\theta\beta}^T$$
$$[H']_{\theta\beta}[U_\theta]+[U_\eta]^T[H']_{\eta\zeta}^T[H']_{\eta\zeta}[U_\eta]+[U_\zeta]^T[H']_{\eta\zeta}^T[H']_{\eta\zeta}[U_\zeta]+$$
$$+(e_z-z_p)([U_\eta]^T[H'']_{\eta\zeta}^T[H]_{\theta\beta}[U_\theta]+[U_\theta]^T[H]_{\theta\beta}^T[H'']_{\eta\zeta}[U_\eta]-$$
$$-(e_y-y_p)([U_\zeta]^T[H'']_{\eta\zeta}^T[H]_{\theta\beta}[U_\theta]+[U_\theta]^T[H]_{\theta\beta}^T[H'']_{\eta\zeta}[U_\zeta])]dx \quad (3)$$

The columns of the nodal values of the transverse displacements are formed from the same elements as in our previous work [27]:

$$\left[U_\eta\right]=\left(\eta_i\ \ \eta_i'\ \ \eta_{i+1}\ \ \eta_{i+1}'\right)^T; \quad (4)$$

$$\left[U_\xi\right]=\left(\xi_i\ \ \xi_i'\ \ \xi_{i+1}\ \ \xi_{i+1}'\right)^T. \quad (5)$$

Columns made up of twist angles and warping measures have a different look - they are added to an intermediate value in the middle of the finite element.

$$\left[U_\theta\right]=\left(\theta_i\ \ \theta_{i+\frac{1}{2}}\ \ \theta_{i+1}\right)^T; \quad (6)$$

$$\left[U_\beta\right]=\left(\beta_i\ \ \beta_{i+\frac{1}{2}}\ \ \beta_{i+1}\right)^T; \quad (7)$$

$$\left[U_{\theta\beta}\right]=\left(\theta_i\ \ \beta_i\ \ \theta_{i+\frac{1}{2}}\ \ \beta_{i+\frac{1}{2}}\ \ \theta_{i+1}\ \ \beta_{i+1}\right)^T. \quad (8)$$

Hermite polynomials for the functions of transverse displacements are assumed to be similar to our previous work [27]:

$$H_1=\frac{2}{l^3}x^3-\frac{3}{l^2}x^2+1;\quad H_2=\frac{x^3}{l^2}-\frac{2}{l}x^2+x;\quad H_3=-\frac{2}{l^3}x^3+\frac{3}{l^2}x^2;\quad H_4=\frac{x^3}{l^2}-\frac{1}{l}x^2. \quad (9)$$

The strings composed of the given Hermite polynomials looks like:

$$\left[H'\right]_{\eta\xi}=\left(\frac{dH_1}{dx}\ \ \frac{dH_2}{dx}\ \ \frac{dH_3}{dx}\ \ \frac{dH_4}{dx}\right); \quad (10)$$

$$\left[H''\right]_{\eta\xi}=\left(\frac{d^2H_1}{dx^2}\ \ \frac{d^2H_2}{dx^2}\ \ \frac{d^2H_3}{dx^2}\ \ \frac{d^2H_4}{dx^2}\right). \quad (11)$$

The Hermite polynomials for the torsion and warping functions in this paper will be quadratic [27]:

$$H_5=1-\frac{3x}{l}+\frac{2x^2}{l^2};\quad H_6=\frac{4x}{l}-\frac{4x^2}{l^2};\quad H_7=-\frac{x}{l}+\frac{2x^2}{l^2} \quad (12)$$

and the corresponding lines are denoted as:

$$\left[H\right]_{\theta\beta}=\left(H_5\ \ H_6\ \ H_7\right); \quad (13)$$

$$\left[H'\right]_{\theta\beta}=\left(\frac{dH_5}{dx}\ \ \frac{dH_6}{dx}\ \ \frac{dH_7}{dx}\right); \quad (14)$$

$$[\Phi]=\left(\frac{dH_5}{dx}\ -H_5\ \frac{dH_6}{dx}\ -H_6\ \frac{dH_7}{dx}\ -H_7\right). \quad (15)$$

Calculating the integrals in (3) by grouping them in accordance with the vector of nodal displacements (2), we get:

$$S=\frac{1}{2}[U]^T([K]-P[G])[U]. \quad (16)$$

P is concentrated load applied at the end of the rod along the x axis at an arbitrary section point with coordinates (e_y, e_z), matrixes [K] and [G] consist of matrices blocks, which we numbered in accordance with the numbering of nodes of a finite element (Figure 1):

$$[K]=\begin{pmatrix}[K_{i,i}] & [K_{i,i+1}]\\ [K_{i+1,i}] & [K_{i+1,i+1}]\end{pmatrix},\ \ [G]=\begin{pmatrix}[G_{i,i}] & [G_{i,i+1}]\\ [G_{i+1,i}] & [G_{i+1,i+1}]\end{pmatrix}, \quad (17)$$

where

$$K_{i,i}=\begin{pmatrix}
\frac{12}{l^3}EI_z & \frac{6}{l^2}EI_z & 0 & 0 & 0 & 0 & 0\\
\frac{6}{l^2}EI_z & \frac{4}{l}EI_z & 0 & 0 & 0 & 0 & 0\\
0 & 0 & \frac{12}{l^3}EI_y & \frac{6}{l^2}EI_y & 0 & 0 & 0\\
0 & 0 & \frac{6}{l^2}EI_y & \frac{4}{l}EI_y & 0 & 0 & 0\\
0 & 0 & 0 & 0 & \frac{7}{3l}GI_x+\frac{7}{3l}GI_\beta & -\frac{1}{2}GI_\beta & -\frac{8}{3l}GI_x-\frac{8}{3l}GI_\beta\\
0 & 0 & 0 & 0 & -\frac{1}{2}GI_\beta & \frac{2l}{15}GI_\beta+\frac{7}{3l}EI_\omega & \frac{2}{3}GI_\beta\\
0 & 0 & 0 & 0 & -\frac{8}{3l}GI_x-\frac{8}{3l}GI_\beta & \frac{2}{3}GI_\beta & \frac{16}{3l}GI_x+\frac{16}{3l}GI_\beta
\end{pmatrix};$$

$$K_{i,i+1}=\begin{pmatrix}
0 & -\frac{12}{l^3}EI_z & \frac{6}{l^2}EI_z & 0 & 0 & 0 & 0\\
0 & -\frac{6}{l^2}EI_z & \frac{2}{l}EI_z & 0 & 0 & 0 & 0\\
0 & 0 & 0 & -\frac{12}{l^3}EI_y & \frac{6}{l^2}EI_y & 0 & 0\\
0 & 0 & 0 & -\frac{6}{l^2}EI_y & \frac{2}{l}EI_y & 0 & 0\\
-\frac{2}{3}GI_\beta & 0 & 0 & 0 & 0 & \frac{1}{3l}(GI_x+GI_\beta) & \frac{1}{6}GI_\beta\\
-\frac{8}{3l}EI_\omega+\frac{l}{15}GI_\beta & 0 & 0 & 0 & 0 & -\frac{1}{6}GI_\beta & -\frac{l}{30}GI_\beta+\frac{1}{3l}EI_\omega\\
0 & 0 & 0 & 0 & 0 & -\frac{8}{3l}EI_\omega-\frac{8}{3l}EI_\beta & -\frac{2}{3}GI_\beta
\end{pmatrix};$$

$$K_{i+1,i+1}=\begin{pmatrix}
\frac{16}{3l}EI_\omega+\frac{8l}{15}GI_\beta & 0 & 0 & 0 & 0 & \frac{2}{3}GI_\beta & -\frac{8}{3l}EI_\omega+\frac{l}{15}GI_\beta \\
0 & \frac{12}{l^3}EI_z & -\frac{6}{l^2}EI_z & 0 & 0 & 0 & 0 \\
0 & -\frac{6}{l^2}EI_z & \frac{4}{l}EI_z & 0 & 0 & 0 & 0 \\
0 & 0 & 0 & \frac{12}{l^3}EI_y & -\frac{6}{l^2}EI_y & 0 & 0 \\
0 & 0 & 0 & -\frac{6}{l^2}EI_y & \frac{4}{l}EI_y & 0 & 0 \\
\frac{2}{3}GI_\beta & 0 & 0 & 0 & 0 & \frac{7}{3l}(GI_x+GI_\beta) & \frac{1}{2}GI_\beta \\
-\frac{8}{3l}EI_\omega+\frac{l}{15}GI_\beta & 0 & 0 & 0 & 0 & \frac{1}{2}GI_\beta & \frac{2l}{15}GI_\beta+\frac{7}{3l}EI_\omega
\end{pmatrix};$$

$$G_{i,i}=\begin{pmatrix}
\frac{6}{5l} & \frac{1}{10} & 0 & 0 & -\frac{(e_z-z_p)}{l} & 0 & 0 \\
\frac{1}{10} & \frac{2l}{15} & 0 & 0 & -\frac{2}{3}e_z+\frac{2}{3}z_p & 0 & -\frac{2}{3}e_z+\frac{2}{3}z_p \\
0 & 0 & \frac{6}{5l} & \frac{1}{10} & \frac{(e_y-y_p)}{l} & 0 & 0 \\
0 & 0 & \frac{1}{10} & \frac{2l}{15} & \frac{2}{3}e_y-\frac{2}{3}y_p & 0 & \frac{2}{3}e_y-\frac{2}{3}y_p \\
-\frac{(e_z-z_p)}{l} & -\frac{2}{3}e_z+\frac{2}{3}z_p & \frac{(e_y-y_p)}{l} & \frac{2}{3}e_y-\frac{2}{3}y_p & \frac{7}{3l}c & 0 & -\frac{16}{6l}c \\
0 & 0 & 0 & 0 & 0 & 0 & 0 \\
0 & -\frac{2}{3}e_z+\frac{2}{3}z_p & 0 & \frac{2}{3}e_y-\frac{2}{3}y_p & -\frac{16}{6l}c & 0 & \frac{16}{6l}c
\end{pmatrix};$$

$$G_{i,i+1}=\begin{pmatrix}
0 & -\frac{6}{5l} & \frac{1}{10} & 0 & 0 & \frac{(e_z-z_p)}{l} & 0 \\
0 & -\frac{1}{10} & -\frac{l}{30} & 0 & 0 & \frac{(e_z-z_p)}{3} & 0 \\
0 & 0 & 0 & -\frac{6}{5l} & \frac{1}{10} & -\frac{(e_y-y_p)}{l} & 0 \\
0 & 0 & 0 & -\frac{1}{10} & -\frac{l}{30} & -\frac{(e_y-y_p)}{3} & 0 \\
0 & \frac{(e_z-z_p)}{l} & -\frac{(e_z-z_p)}{3} & -\frac{(e_y-y_p)}{l} & \frac{(e_y-y_p)}{3} & \frac{2c}{6l} & 0 \\
0 & 0 & 0 & 0 & 0 & 0 & 0 \\
0 & 0 & \frac{2(e_z-z_p)}{3} & 0 & -\frac{2(e_y-y_p)}{3} & \frac{16c}{6l} & 0
\end{pmatrix};$$

$$G_{i+1,i+1}=\begin{pmatrix} 0 & 0 & 0 & 0 & 0 & 0 & 0 \\ 0 & \frac{6}{5l} & -\frac{1}{10} & 0 & 0 & -\frac{(e_z-z_p)}{l} & 0 \\ 0 & -\frac{1}{10} & \frac{2l}{15} & 0 & 0 & \frac{2}{3}e_z-\frac{2}{3}z_p & 0 \\ 0 & 0 & 0 & \frac{6}{5l} & -\frac{1}{10} & \frac{(e_y-y_p)}{l} & 0 \\ 0 & 0 & 0 & -\frac{1}{10} & \frac{2l}{15} & -\frac{2}{3}e_y+\frac{2}{3}y_p & 0 \\ 0 & -\frac{(e_z-z_p)}{l} & \frac{2}{3}e_z-\frac{2}{3}z_p & \frac{(e_y-y_p)}{l} & -\frac{2}{3}e_y+\frac{2}{3}y_p & \frac{7c}{3l} & 0 \\ 0 & 0 & 0 & 0 & 0 & 0 & 0 \end{pmatrix};$$

$$c=\left(r_p^2+e_zb_z+e_yb_y+\omega_Ab_\omega\right). \quad (18)$$

Matrices [K] and [G] are symmetric therefore equalities (19) are fulfilled:

$$\left[K_{i,i+1}\right]=\left[K_{i+1,i}\right]^T;\quad \left[G_{i,i+1}\right]=\left[G_{i+1,i}\right]^T. \quad (19)$$

3. Results and Discussion

For the numerical solution of the problem, we consider a thin-walled rods of open profile (warped (Figure 2) and non-warped (Figure 3)) and closed profile (Figure 4). Rod length L_1 = 5 m for profile 1 and rod length $L_{2,3}$ = 3 m for profiles 2 and 3.

Kinematic boundary conditions:

In the first case: $\eta_1 = \zeta_1 = \theta_1 = \eta_n = \zeta_n = \theta_n = 0$ (hinge support, prohibitive translational motion (non-axial longitudinal rods) и rotational motion relative to the rods longitudinal axis;

In the second case: $\eta_1 = \eta_1' = \zeta_1 = \zeta_1' = \theta_1 = \beta_1 = 0$ (hard pinch at one end).

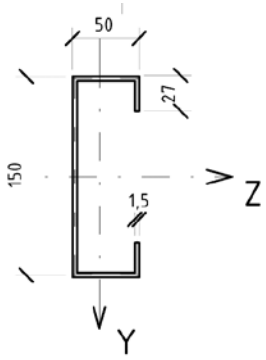

Figure 2. Shape 1.

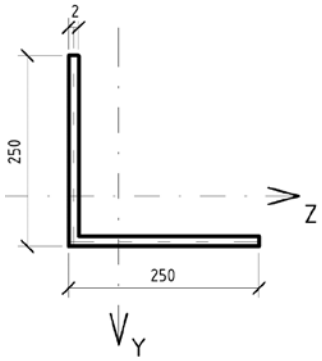

Figure 3. Shape 2.

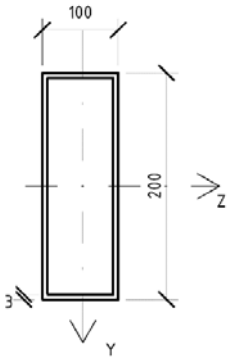

Figure 4. Shape 3.

Rod material - steel C245:

Physical characteristics of steel C245: E = 20600 kN/cm², G = 7920 kN/cm².

Table 1. Geometric characteristics of the rod section.

I_z	I_y	I_x	I_ω	I_β	e_z	e_y	z_p	y_p	b_ω	b_z	b_y	r_p^2
cm⁴	cm⁴	cm⁴	cm⁶	cm⁴	cm	cm	cm	cm	cm	cm	cm	cm²
						Shape 1						
18.767	152.964	0.034	1137	203	0	0	-2.8	0	0	8.253	0	45.5
						Shape 2						
651	651	0.133	0	0	0	0	0	0	0	0	0	130
						Shape 3						
947	324	745	1553	78	0	0	0	0	0	0	0	72

Solve the basic resolving stability equation for compressed rods:

$$\det([K]-P[G])=0. \quad (20)$$

Determine the smallest solution that corresponds to the critical force for the given number of FE and for given kinematic boundary conditions. The tables below compare the results obtained in the numerical solution of problems with different types of approximation to each other. The numerical solutions are compared with analytical solutions. Numerical solutions for linear approximation are obtained based on the results in [27].

Table. 2 Magnitude of critical forces P^{ij} (i – shape, j – anchor) for two types of approximation of the functions of the twist angle and the θ and β deplanation with a different number of FE.

	2	4	8	16	32	64
P_{lin}^{11} [27], kN	15.373	15.250	15.180	14.955	14.378	13.636
P_{quad}^{11}, kN	13.548	13.154	13.065	13.044	13.0413	13.039
Analytical solutions P^{11}, kN						
P_{Euler}^{an}, kN	15.247					
P_{Vlasov}^{an}, kN	13.039					
P_{lin}^{12} [27], kN	3.817	3.815	3.813	3.808	3.797	3.785
P_{quad}^{12}, kN	3.788	3.780	3.778	3.777	3.777	3.777
Analytical solutions P^{12} kN						
P_{Euler}^{an}, kN	3.811					
P_{Vlasov}^{an}, kN	3.777					
$P_{lin}^{21(22)}$ [27], kN	8.1028					
$P_{quad}^{21(22)}$, kN						
Analytical solutions $P^{21(22)}$, kN						
P_{Euler}^{an}, kN	1469.146					
P_{Vlasov}^{an}, kN	8.1028					
P_{lin}^{32} [27], kN	183.076	182.988	182.983	182.983	182.983	182.983
P_{quad}^{32}, kN	183.076	182.988	182.983	182.983	182.983	182.983
Analytical solutions P^{32}, kN						
P_{Euler}^{an}, kN	182.983					
P_{Vlasov}^{an}, kN						
P_{lin}^{31} [27], kN	737.436	732.305	731.954	731.931	731.930	731.930
P_{quad}^{31}, kN	737.436	732.305	731.954	731.931	731.930	731.930
Analytical solutions P^{31}, kN						
P_{Euler}^{an}, kN	731.930					
P_{Vlasov}^{an}, kN						

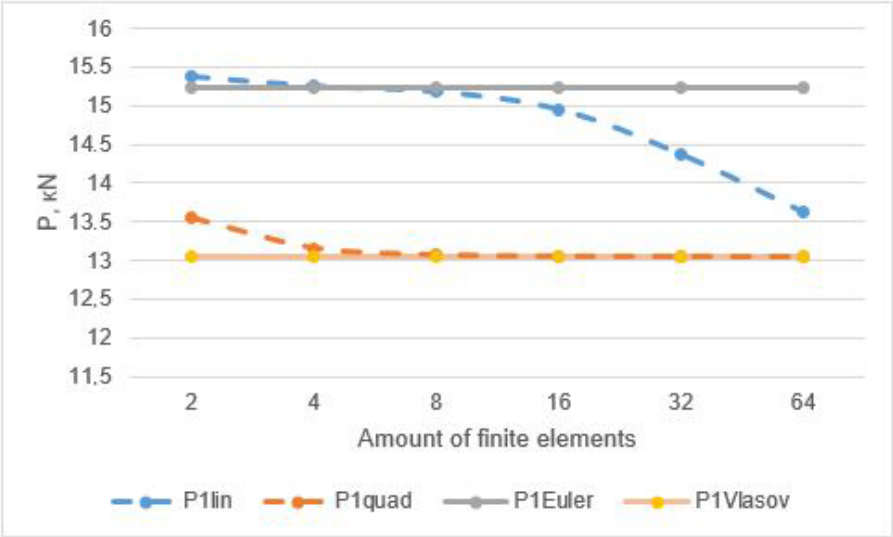

Figure 5. Graph of P_{11} versus the number of finite elements and the type of approximation of functions θ and β.

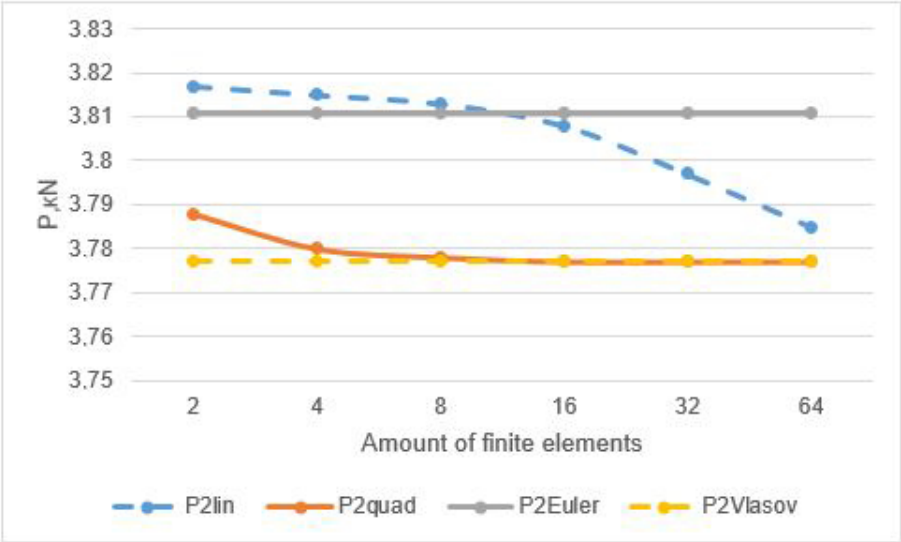

Figure 6. Graph of P_{12} versus the number of finite elements and the type of approximation of functions θ and β.

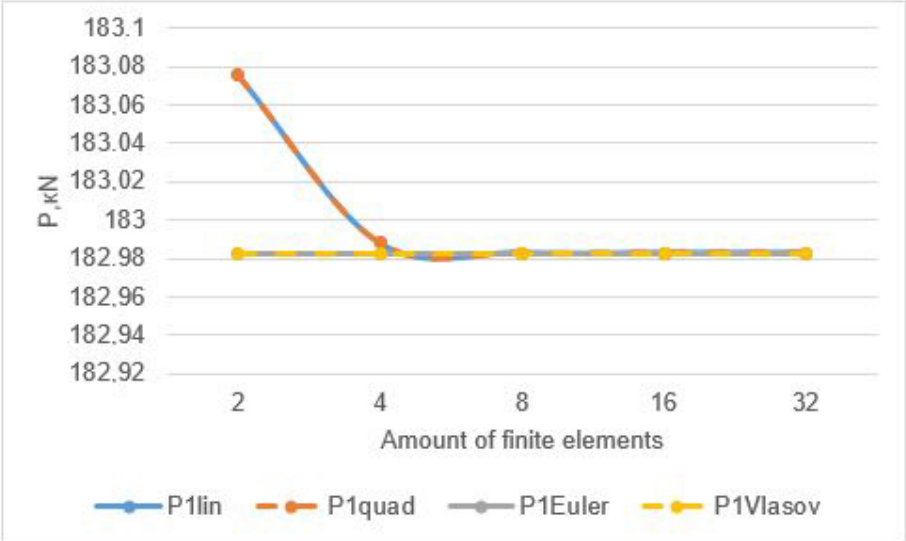

Figure 7. Graph of P_{32} versus the number of finite elements and the type of approximation of the functions θ and β.

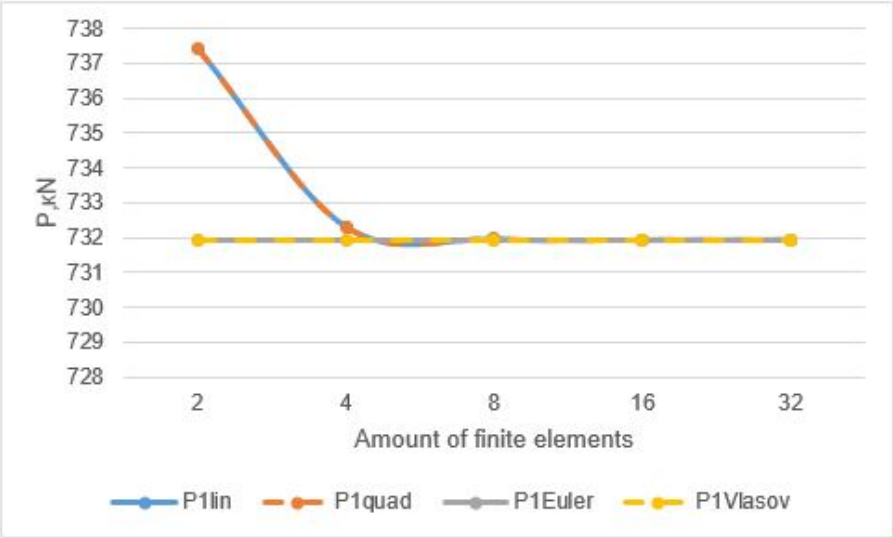

Figure 8. Graph of P_{31} versus the number of finite elements and the type of approximation of the functions θ and β.

Determination of the critical force of a hinge-supported [28] rod having a profile 1:

$$(P_z - P)(P_y - P)(P_\omega - P)\cdot r_p^2 - y_p^2 \cdot P^2 \cdot (P_z - P) - z_p^2 \cdot P^2 \cdot (P_y - P) = 0, \quad (21)$$

where

$$P_z = \frac{\pi^2}{L^2}\cdot EI_z = 15.262 \text{ кN}; \quad P_y = \frac{\pi^2}{L^2}\cdot EI_y = 124.273 \text{ кN}; \quad P_\omega = \frac{\frac{\pi^2}{L^2}\cdot EI_\omega + GI_x}{r_p^2} = 26.220 \text{ кN}; \quad (22)$$

r_p, y_p , z_p are polar radius of inertia relative to the center of the bend and coordinates of the center of the bend

From (21) $P_{\min}$ = 13.039 кN.

The critical forces obtained in the calculation of thin-walled rods having a profile of 1 under two types of kinematic boundary conditions correspond to the flexural-torsional form of buckling. Approximation by quadratic functions turns out to be faster in cases where the buckling has a flexural-torsional form. At 2 finite elements, the quadratic approximation reaches a value more precisely than at 64 finite elements, the linear approximation.

Analyzing the results of calculating the L-profile, we conclude that the values of the critical forces obtained by linear and quadratic approximations coincide in magnitude with the analytical value according to Vlasov [24] under any kinematic boundary conditions. The shape of the loss of stability in such a profile and at such geometric dimensions is a purely torsional (Figure 9). The value of the critical force according to Euler corresponds to the bending form of buckling and is given for reference.

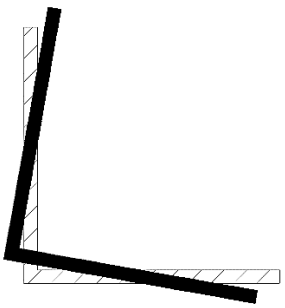

Figure 9. Purely torsional form of stability loss of the rod(L-section).

According to the results obtained, it is clear that the form of buckling of the box-shaped profile is purely bending. The order of approximation of the functions of the torsion forms and measures of deplanation is unimportant.

The critical load values were also compared with the Euler buckling loads. The results showed that taking warping into account reduces the critical load for the open cross sections (C-section, L-section) but doesn't have a significant impact on the closed cross-section (rectangular pipe).

The problem of spatial problems for systems of thin-walled rods has not been solved to date, and therefore the results obtained today cannot extend to spatial and even planar problems. However, as soon as the problem of turning the deplanation and bimoment measures is resolved, the results presented in the article will automatically be transferred to thin-walled rod systems.

4. Conclusions

1. A geometric stiffness matrix of a thin-walled rod was obtained for a cubic approximation of the functions of transverse displacements and quadratic approximation of the torsion functions and deplanation.

2. With the help of the constructed matrix, using FEM the critical load was determined for the bar with both ends pinned and different types of the cross section (C-section, L-section and the rectangular pipe).

3. The critical load values were also compared with the Euler buckling loads. The results showed that taking warping into account reduces the critical load for the open cross sections (C-section, L-section) but doesn't have a significant impact on the closed cross-section (rectangular pipe).

4. Approximation by quadratic functions turns out to be faster in cases where the buckling has a flexural-torsional form. At 2 finite elements, the quadratic approximation reaches a value more precisely than at 64 finite elements, the linear approximation. In cases where the form of buckling is purely torsional or flexural, there are no advantages in no approximation method.

5. The constructed geometrical stiffness matrix is acceptable to solve buckling problems of the thin-walled bars for both open and closed cross sections.

References

1. Pichugin, S.F. Reliability estimation of industrial building structures. Magazine of Civil Engineering. 2018. 83(7). Pp. 24–37. DOI: 10.18720/MCE.83.3.
2. Kirsanov, M.N. Analytical calculation of the frame with an arbitrary number of panels. Magazine of Civil Engineering. 2018. 82(6). Pp. 127–135. DOI: 10.18720/MCE.82.12.
3. Kirsanov, M.N. Installation diagram of the lattice truss with an arbitrary number of panels. Magazine of Civil Engineering. 2018. 81(5). Pp. 174–182. DOI: 10.18720/MCE.81.17.
4. Trubina, D., Abdulaev, D., Pichugin, E., Rybakov, V., Garifullin, M., Sokolova, O. Comparison of the Bearing Capacity of LST- Profile Depending on the Thickness of its Elements. Applied Mechanics and Materials. 2015. Vol. 725–726. Pp. 752–757.
5. Rybakov, V.A., Gamayunova, O.S. The stress-strain state of frame constructions elements from thin-walled cores. Construction of Unique Buildings and Structures. 2013. No. 7(12). Pp. 79–123.
6. Askinazi, V.Yu. Prostranstvennaya ustoychivost elementov stalnykh ramnykh konstruktsiy peremennoy zhestkosti [Spatial stability of elements of steel frame structures of variable stiffness]. Doctorial Thesis. SPb., 2017. (rus)
7. Belyy, A.G. Deformatsionnyy raschet i ustoychivost tonkostennykh prizmaticheskikh sterzhney proizvolnogo profilya szhatykh s dvukhosnym ekstsentrisitetom [Deformation calculation and stability of thin-walled prismatic rods in a compression profile compressed with a biaxial eccentricity]. PhD Thesis. SPb.: SPbGASU, 2000. 114 p. (rus)
8. Moen, C.D., Schafer, B.W. Elastic buckling of cold-formed steel columns and beams with holes. Engineering Structures. 2009. Vol. 31. No. 12. Pp. 2812–2824.
9. Vieira, R., Virtuoso, F., Pereira, E. Buckling of thin-walled structures through a higher order beam model. Computers & Structures. 2017. Vol. 180. Pp. 104–116.
10. Samanta, A., Kumar, A. Distortional buckling in monosymmetric I-beams. Thin-walled structures. 2006. Vol. 44. No. 1. Pp. 51–56.
11. Tuyev, D.S., Umnova, O.V. Vliyaniye mestnoy poteri ustoychivosti na nesushchuyu sposobnost lstk profilya [The effect of local buckling on the load-carrying capacity of a profile sheet]. In the collection: New information technologies in science. Collection of articles of the international scientific-practical conference. 2016. Pp. 177–184. (rus)
12. Trubina, D.A., Kononova, L.A., Kaurov, A.A., Pichugin, Y.D., Abdulaev, D.A. Local buckling of steel cold-formed profiles under transverse bending. Construction of Unique Buildings and Structures. 2014. 19(4). (rus)
13. Trouncer, A.N., Rasmussen, K.J.R. Flexural–torsional buckling of ultra light-gauge steel storage rack uprights. Thin-Walled Structures. 2014. Vol. 81. Pp. 159–174.
14. Sastry, S.Y.B., Krishna, Y., Koduganti, A. Flexural buckling analysis ofthin walled lipped channel cross section beams with variable geometry. International Journal of Innovative Research in Science. Engineering and Technology. 2014. Vol. 3. No. 6. Pp. 13484–13494.
15. Rybakov, V.A. Primeneniye polusdvigovoy teorii V.I. Slivkera dlya analiza napryazhenno-deformirovannogo sostoyaniya sistem tonkostennykh sterzhney [Application of the semi-shear theory V.I. Slivker for the analysis of the stress-strain state of systems of thin-walled rods]. Phd Thesis. SPb., 2012. 184 p. (rus)
16. Dyakov, S.F. Primeneniye polusdvigovoy teorii V.I. Slivkera k resheniyu zadach statiki i dinamiki tonkostennykh sterzhney [Application of the semi-shear theory V.I. Slivker to solve problems of statics and dynamics of thin-walled rods]. PhD Thesis. SPb., 2013. 147 p. (rus)
17. Lalin, V., Rybakov, V., Sergey, A. The finite elements for design of frame of thin-walled beams. Applied Mechanics and Materials. 2014. Vol. 578–579. Pp. 858–863.
18. Tyukalov, Yu.Ya. Refined finite element of rods for stability calculation. Magazine of Civil Engineering. 2018. 79(3). Pp. 54–65. DOI: 10.18720/MCE.79.6.

19. Garifullin, M., Bronzova, M., Heinisuo, M., Mela, K., Pajunen, S. Cold-formed RHS T joints with initial geometrical imperfections. Magazine of Civil Engineering. 2018. 80(4). Pp. 81–94. DOI: 10.18720/MCE.80.8 (rus)
20. Atavin, I.V., Melnikov, B.E., Semenov, A.S., Chernysheva, N.V., Yakovleva, E.L. Influence of stiffness of node on stability and strength of thin-walled structure. Magazine of Civil Engineering. 2018. 8(4). Pp. 48–61. DOI: 10.18720/MCE.80.5
21. Tusnina, V.M. Semi-rigid steel beam-to-column connections. Magazine of Civil Engineering. 2017. No. 5. Pp. 25–39. DOI: 10.18720/MCE.73.3.
22. Marchenko, T.V., Bannikov, D.O. Sopostavitelnyy analiz form poteri ustoychivosti tonkostennykh sterzhnevykh elementov [Comparative analysis of the forms of buckling of thin-walled core elements]. Steel Construction. 2009. Vol. 15. No. 3. Pp. 177–188. (rus)
23. Perelmuter, A.V., Slivker, V.I. Structural equilibrium stability and related problems. Vol. 1. SCAD SOFT, 2007. 670 p. (rus)
24. Slivker, V.I. Structural mechanics. Variational basis. ASV, 2005. 736 p. (rus)
25. Perelmuter, A.V., Slivker, V.I. Design models of structures and the possibility of their analysis. Kiev: Steel, 2002. 600 p. (rus)
26. Haidarali, M.R., Nethercot, D.A. Finite element modelling of cold-formed steel beams under local buckling or combined local/distortional buckling. Thin-Walled Structures. 2011. Vol. 49. No. 12. Pp. 1554–1562.
27. Lalin, V.V., Rybakov, V.A., Dyakov, S.F., Kudinov, V.V., Orlova, Ye.S. Polusdvigovaya teoriya V.I. Slivkera v zadachakh ustoychivosti tonkostennykh sterzhney. Inzhenerno-stroitelnyy zhurnal. 2019. No. 3(87). Pp. 66–79. DOI: 10.18720/MCE.87.6
28. Vlasov, V.Z. Thin-walled elastic rods. Fizmatgis, 1959. 574 p.

Contacts:

Vladimir Rybakov, +7(964)3312915; fishermanoff@mail.ru
Vladimir Lalin, +7(921)3199878; vllalin@yandex.ru
Sergey Ivanov, +7(904)5567654; serzikserzik@gmail.com
Artur Azarov, +7(905)2705646; alexio009@mail.ru

Инженерно-строительный журнал

ISSN 2071-0305

сайт журнала: http://engstroy.spbstu.ru/

DOI: 10.18720/MCE.89.10

Квадратичная аппроксимация функций форм в полусдвиговой теории устойчивости В.И. Сливкера

В.А. Рыбаков, В.В. Лалин, С.С. Иванов, А.А. Азаров*

Санкт-Петербургский политехнический университет Петра Великого, Санкт-Петербург, Россия

** E-mail: alexio009@mail.ru*

Ключевые слова: тонкостенные стержни, полусдвиговая теория Сливкера, теория устойчивости, функционал устойчивости, полиномы Эрмита, функции формы

Аннотация. Поскольку потеря несущей способности некоторых сжатых элементов конструкций из ЛСТК происходит при общей потере устойчивости и для некоторых из них нет аналитического решения, представляется особо интересным рассмотрение вариационной постановки задачи и численное ее решение. В данном исследовании были получены матрицы жесткости и геометрической жесткости при квадратичной вариации полиномов Эрмита, аппроксимирующих функции угла закручивания и депланации. Получены зависимости критической нагрузки от количества КЭ для разных геометрических и кинематических граничных условий. Показана несостоятельность аппроксимации линейными функциями форм по сравнению с квадратичной аппроксимацией, которая оказывается оптимальной, так как практически сразу достигает точного аналитического решения, при изгибно-крутильной форме потери устойчивости. Для чисто крутильной или изгибной формы потери устойчивости показано, что аппроксимация функций угла закручивания и депланации при различных полиномах Эрмита не дает более быстрой сходимости.

Литература

1. Пичугин С.Ф. Оценка надежности конструкций промышленных зданий // Инженерно-строительный журнал. 2018. № 7(83). С. 24–37. DOI: 10.18720/MCE.83.3.
2. Кирсанов М.Н. Аналитический расчет рамы с произвольным числом панелей // Инженерно-строительный журнал. 2018. № 6(82). С. 127–135. DOI: 10.18720/MCE.82.12.
3. Кирсанов М.Н. Монтажная схема решетчатой фермы с произвольным числом панелей // Инженерно-строительный журнал. 2018. № 5(81). С. 174–182. DOI: 10.18720/MCE.81.17.
4. Trubina D., Abdulaev D., Pichugin E., Rybakov V., Garifullin M., Sokolova O. Comparison of the Bearing Capacity of LST- Profile Depending on the Thickness of its Elements // Applied Mechanics and Materials. 2015. Vol. 725-726. Pp. 752–757.
5. Рыбаков В.А., Гамаюнова О.С. Напряженно-деформированное состояние элементов каркасных сооружений из тонкостенных стержней // Строительство уникальных зданий и сооружений. 2013. № 7(12). С. 79–123.
6. Аскинази В.Ю. Пространственная устойчивость элементов стальных рамных конструкций переменной жесткости: автореф. дис. ... канд. техн. наук. СПб., 2017.
7. Белый А.Г. Деформационный расчет и устойчивость тонкостенных призматических стержней произвольного профиля сжатых с двухосным эксцентриситетом: автореф. дис. … канд. техн. наук. СПб.: СПбГАСУ, 2000. 114 с.
8. Moen C.D., Schafer B.W. Elastic buckling of cold-formed steel columns and beams with holes // Engineering Structures. 2009. Vol. 31. No. 12. Pp. 2812–2824.
9. Vieira R., Virtuoso F., Pereira E. Buckling of thin-walled structures through a higher order beam model // Computers & Structures. 2017. Vol. 180. Pp. 104–116.
10. Samanta A., Kumar A. Distortional buckling in monosymmetric I-beams // Thin-walled structures. 2006. Vol. 44. No. 1. Pp. 51–56.
11. Туев Д.С., Умнова О.В. Влияние местной потери устойчивости на несущую способность лстк профиля // Новые информационные технологии в науке: сб. статей Междунар. науч.-практ. конф.. 2016. С. 177–184.
12. Туев Д.С., Умнова О.В. Влияние местной потери устойчивости на несущую способность лстк профиля // Новые информационные технологии в науке: сб. статей Междунар. науч.-практ. конф., 2016. С. 177–184.
13. Trouncer A.N., Rasmussen K.J.R. Flexural–torsional buckling of ultra light-gauge steel storage rack uprights // Thin-Walled Structures. 2014. Vol. 81. Pp. 159–174.
14. Sastry S.Y.B., Krishna Y., Koduganti A. Flexural buckling analysis ofthin walled lipped channel cross section beams with variable geometry // International Journal of Innovative Research in Science, Engineering and Technology. 2014. Vol. 3. No. 6. Pp. 13484–13494.
15. Рыбаков В.А. Применение полусдвиговой теории В.И. Сливкера для анализа напряженно-деформированного состояния систем тонкостенных стержней: дис. … канд. техн. наук. СПб., 2012. 184 с.

16. Дьяков С.Ф. Применение полусдвиговой теории В.И. Сливкера к решению задач статики и динамики тонкостенных стержней: дис. … канд. техн. наук. СПб., 2013. 147 с.
17. Lalin V., Rybakov V., Sergey A. The finite elements for design of frame of thin-walled beams // Applied Mechanics and Materials. 2014. Vol. 578-579. Pp. 858–863.
18. Тюкалов Ю.Я. Улучшенный стержневой конечный элемент для решения задач устойчивости // Инженерно-строительный журнал. 2018. № 3(79). С. 54–65. DOI: 10.18720/MCE.79.6.
19. Гарифуллин М.Р., Бронзова М.К., Хейнисуо М., Мэла К., Паюнен С. Сварные узлы холодногнутых труб прямоугольного сечения с начальными несовершенствами // Инженерно-строительный журнал. 2018. № 4(80). С. 81–94. DOI: 10.18720/MCE.80.8.
20. Атавин И.В., Мелников Б.Е., Семенов А.С., Чернышева Н.В., Яковлева Е.Л. Влияние жесткости узловых соединений на устойчивость и прочность тонкостенных конструкций // Инженерно-строительный журнал. 2018. 8(4). С. 48–61. DOI: 10.18720/MCE.80.5
21. Туснина В.М. Податливые соединения стальных балок с колоннами // Инженерно-строительный журнал. 2017. № 5(73). С. 25–39. DOI: 10.18720/MCE.73.3.
22. Марченко Т.В., Банников Д.О. Сопоставительный анализ форм потери устойчивости тонкостенных стержневых элементов // Металлические конструкции. 2009. Т. 15. № 3. С. 177–188.
23. Перельмутер А.В., Сливкер В.И. Устойчивость равновесия конструкций и родственные проблемы. Т. 1. М.: Изд-во СКАД СОФТ, 2007. 670 с.
24. Сливкер В.И. Строительная механика. Вариационные основы.: Изд-во АСВ, 2005. 736 с
25. Перельмутер А.В., Сливкер В.И. Расчетные модели сооружений и возможность их анализа. Киев: Изд-во Сталь, 2005. 600 с.
26. Haidarali M.R., Nethercot D.A. Finite element modelling of cold-formed steel beams under local buckling or combined local distortional buckling // Thin-Walled Structures. 2011. Vol. 49. No. 12. Pp. 1554–1562.
27. Лалин В.В., Рыбаков В.А., Дьяков С.Ф., Кудинов В.В., Орлова Е.С. Полусдвиговая теория В.И. Сливкера в задачах устойчивости тонкостенных стержней // Инженерно-строительный журнал. 2019. № 3(87). С. 66–79. DOI: 10.18720/MCE.87.6
28. Власов В.З. Тонкостенные упругие стержни. М.: Физматлит, 1959. 574 с.

Контактные данные:

Владимир Александрович Рыбаков, +7(964)3312915; эл. почта: fishermanoff@mail.ru
Владимир Владимирович Лалин, +7(921)3199878; эл. почта: vllalin@yandex.ru
Сергей Сергеевич Иванов, +7(904)5567654; эл. почта: serzikserzik@gmail.com
Артур Александрович Азаров, +7(905)2705646; эл. почта: alexio009@mail.ru